Nuclear Physics A519 (1990) 141c-156c
North-Holland

COLLECTIVE FLOW, MULTI-FRAGMENT EMISSION AND AZIMUTHAL ASYMMETRIES IN INTERMEDIATE ENERGY NUCLEUS-NUCLEUS COLLISIONS[a]

G.D. WESTFALL, C.A. Ogilvie, D.A. Cebra, W.K. Wilson, A. Vander Molen, W. Bauer, J.S. Winfield, D. Krofcheck, J. Karn, S. Howden, T. Li, R. Lacey, K. Tyson, and M. Cronqvist

National Superconducting Cyclotron Laboratory and
Department of Physics and Astronomy
Michigan State University, East Lansing, MI 48824-1321, USA

and

A. Nadasen
Department of Physics
University of Michigan at Dearborn, Dearborn, MI 48128, USA

Using the MSU 4π Array with the NSCL K1200 Superconducting Cyclotron we have measured an excitation function for $^{40}Ar+^{51}V$ from 35 to 100 MeV/nucleon. We have observed a minimum in collective flow around 82 MeV/nucleon which marks the transition from attractive to repulsive scattering. Multi-fragment emission is observed to occur sequentially in reactions at 35 MeV/nucleon. As the beam energy is raised, the emission becomes more simultaneous. Using azimuthal asymmetries, we have extracted rotation-like phenomena. This signal for rotation is strong at 35 MeV/nucleon and nearly disappears as the beam energy is raised to 85 MeV/nucleon.

1. INTRODUCTION

Collisions of nuclei at intermediate energies (20 - 200 MeV/nucleon) provide the opportunity of studying nuclear matter at densities up to twice nuclear matter density and at excitations up to 50 MeV/nucleon. This information concerning the nuclear equation of state (EOS) can be gathered in an environment that is less disturbed by the thermal fluctuations and pion production that are evident at energies around 1 GeV/nucleon. At lower energies ($\simeq$ 20 MeV/nucleon) the interaction between two nuclei is dominantly attractive[1] while at higher energies ($\simeq$ 200 MeV/nucleon) nucleon-nucleon scattering becomes increasingly important leading to a repulsive interaction. Several groups have studied in detail the phenomena of collective flow at energies from 200 to 1000 MeV/nucleon.[2-6]. We term the

[a]This was supported by the National Science Foundation Grant No. PHY 89-13815.

energy at which the dominant interaction changes from attractive to repulsive as the balance energy, E_{bal}. A prediction of E_{bal} using the Boltzmann-Uehling-Uhlenbeck model[7-14] (BUU) involves the interplay between the mean-field interaction and nucleon-nucleon scattering. Thus in principle the determination of E_{bal} may provide clues to the EOS. However, we will show that although E_{bal} is sensitive to the EOS, it is more sensitive to the assumed nucleon-nucleon scattering of the BUU model[15-17].

In the reactions addressed here, many fragments ($\simeq$ 10) are emitted in central collisions. The question of how the system emits these fragments bears on the ability of the experimenter to determine the reaction mechanisms involved well enough to extract information about the EOS. One extreme idea for the disassembly of the system is that the system emits particles completely sequentially, recoiling and equilibrating after each particle is emitted. The opposite extreme is that the system emits all of its fragments simultaneously in a violent explosion. These two ideas produce different kinematic correlations between the emitted fragments leading to observable differences. The method we chose[18] to study the question of the time-scales of emission is event shape analysis using sphericity/coplanarity parameters[19,20]. This method provides the experimenter with a measure of the shape of the event in momentum space. By comparing our experimental results for sphericity/coplanarity with a simulation incorporating the two assumptions of sequential and simultaneous emission, we determined that at 35 MeV/nucleon, the observed fragments are emitted sequentially. As the beam energy is raised, the observed emission pattern becomes less sequential although not completely simultaneous.

Another method to probe the details of the reaction mechanisms in intermediate energy nucleus-nucleus collisions is that of azimuthal asymmetries[21]. By determining the relative yields of particles with respect to the reaction plane, phenomena such as collective flow and rotation become evident. Rotation is characterized by an in-plane enhancement of fragment emission while collective flow is seen by studying fragment emission with respect to the direction of the projectile. We observe that at 35 MeV/nucleon there is a strong signal of rotation-like phenomena and the collective flow described above. This rotation decreases with increasing beam energy and almost disappears at 85 MeV/nucleon.

2. DETECTION APPARATUS

The results presented here were obtained using the MSU 4π Array[22] in its Mark I configuration consisting of 170 fast/slow plastic phoswich scintillator detectors arranged in 30 subarrays along with a forward array composed of 45 phoswich counters of similar design. The main ball counters had a 3 mm thick fast plastic ΔE backed by a 30 cm thick slow plastic E counter and covered angles from 20° to 160°. The dynamic range of these detectors was set so that fragments up to Z=4 were accepted. The forward array detectors had a 1.6 mm thick ΔE and a 13 cm E and the dynamic range was set to accept up to Z=18. The forward array covered angles from 7° to 20°. Thus the entire system was composed of 215

phoswich counters covering 85% of 4π. A schematic representation of the MSU 4π Array is shown in Fig. 1.

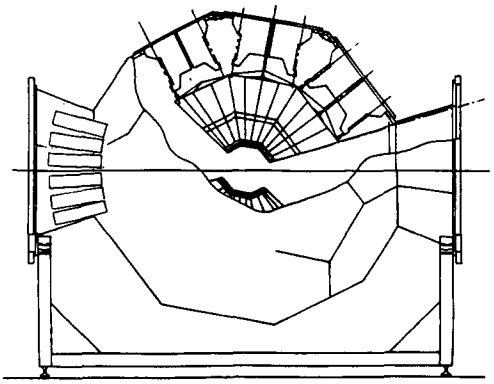

Figure 1: Schematic drawing of the MSU 4π Array showing the location of the forward array.

The event trigger consisted of the multiplicity of detectors firing. Minimum bias triggers (one or more counter firing) and higher multiplicity triggers were recorded at 7 beam energies; 35, 45, 55, 65, 75, 85, and 100 MeV/nucleon. The target consisted of a 3.3 mg/cm^2 natural vanadium foil.

3. RESULTS

3.1 Event topography

In order to extract detailed information from intermediate energy nucleus-nucleus collisions, the events must be characterized as completely as possible[23]. This characterization includes the impact parameter, b, and the reaction plane. To gain insight into our ability to characterize events with the 4π Array, we used an event simulator, FREESCO[19,24], filtered through the acceptance of the Array. Thus we were able to test various methods of determining the impact parameter and the reaction plane and to choose the ones most suited to our apparatus.

The method we chose for determining the impact parameter was to measure the amount of midrapidity charge, Z_{mr}. Midrapidity charge is defined as the sum of the observed charge with rapidity $0.75y_t \leq y \leq 0.75y_p$ in the center-of-mass frame. This method of determining the impact parameter does not depend on the details of the decay process as a bound lithium fragment observed at midrapidity contributes to Z_{mr} the same as three midrapidity protons. In Fig. 2 we show the percentage of events as a function of the impact parameter divided by the maximum impact parameter, b_{max}, for four bins in Z_{mr} corresponding to central, midcentral, midperipheral, and peripheral collisions. Note that for central collisions the maximum of the distribution occurs around $b/b_{max} = 0.3$.

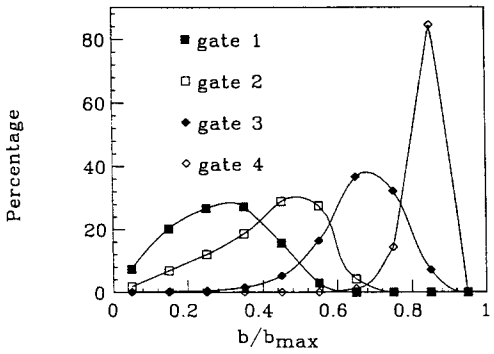

Figure 2: Percentage of events falling into four impact parameter bins from FREESCO simulations passed through the acceptance filter.

To determine the reaction plane, we use a new method[17,21] that is sensitive not only to collective motion in the reaction plane but also to other collective motion such as rotation. The commonly used method of determining the reaction plane devised by Danielewicz and Odyniec[25] depends on the existence of collective flow in the reaction plane. Their method would not be able to determine a reaction plane well for the case where rotation dominates. In the new method, the reaction plane is found by taking the p_z axis along the beam axis, projecting the event onto the p_x-p_y plane, and fitting a line through the origin and the (p_x,p_y) values for all the particles. This line is taken as the intersection of the reaction plane and the p_x-p_y plane. The method of Danielewicz and Odyniec is then used to determine which half of the reaction plane is associated with the projectile fragments. In Fig. 3 a histogram of the difference between the azimuthal angle of the determined reaction plane and the known reaction plane is shown for a FREESCO simulation of 70 MeV/nucleon Ca+Ca passed through the acceptance filter of the 4π Array. Note that this method gives results that are very similar to the method of Danielewicz and Odyniec when strong collective flow is present.

3.2 Collective flow

Collective flow or directed transverse momentum occurs when the average transverse momentum for fragments emitted in the forward hemisphere is opposite to that for fragments emitted in the backward hemisphere in the center-of-mass frame. At low energies, the interaction between two nuclei is dominantly attractive and deflects the forward going fragments to negative scattering angles. At high energies, the interaction is dominantly repulsive and scatters fragments to positive angles. The incident energy at which the interaction changes from attractive to repulsive is termed E_{bal}. This observable has the advantage that it can be compared with the results of microscopic transport models more directly than other ob-

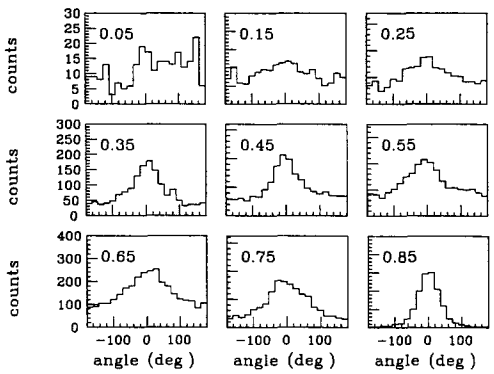

Figure 3: Difference of the azimuthal angle between the found and known reaction planes for events simulated with FREESCO for 70 MeV/nucleon Ca+Ca filtered through the acceptance of the 4π Array.

servables such as the magnitude of the collective flow. For example, it is not necessary for the model to describe composite nucleus production or for the experiment to correct for the lack of precision in determining the reaction plane.

The observable for collective flow is a positive quantity for both positive and negative angle scattering. This result stems from the method of determining the direction of the flow in terms of the vector $\vec{Q}$ which is defined as[25]

$$\vec{Q} = \sum_{j \neq i}^{N} \omega_j \vec{p}_j^{\perp}. \tag{1}$$

This vector will lie in the reaction plane if there is collective flow. Here $\vec{p}_j^{\perp}$ is the transverse momentum of the j^{th} particle, N is the number of particles, ω_j is a weighting factor, and $\vec{p}_j^{\perp}$ is the perpendicular momentum of each particle. The factor ω_j is given by $\omega_j = \frac{p_j^z}{|p_j^z|}$ which corresponds to positive for forward going particles and negative for backward going particles in the center-of-mass. Thus $\vec{Q}$ will point in the direction of the directed transverse momentum and the slope of the average transverse momentum in the reaction plane as a function of rapidity will always be positive. Thus the transition from negative angle scattering to positive angle scattering will manifest itself in terms of the collective flow going through zero as a function of incident energy.

To minimize distortion of the collective flow due to detector acceptance, we will plot the average transverse momentum in the reaction plane divided by the total transverse momentum, $< p^x/p^{\perp} >$ as a function of the rapidity in the center-of-mass. We define the

reduced flow as d< $p^x/p^\perp$ >/dy. This reduced flow will be used to determine E_{bal}. In Fig. 4, < $p^x/p^\perp$ > versus y is plotted for protons from non-peripheral collisions of Ar+V at 45

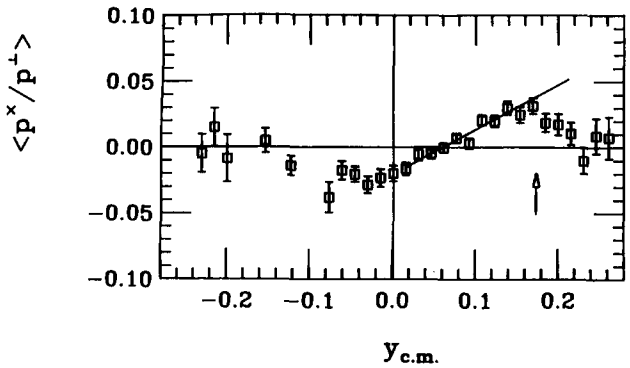

Figure 4: Average transverse momentum versus rapidity in the center-of-mass for protons from 45 MeV/nucleon Ar+V.

MeV/nucleon.

The reduced flow is determined from y=0 to y=0.8y_p in the center-of-mass for five fragment types at the seven incident energies. These flow values are shown in Fig. 5 for mid-central collisions. Note that there is a clear minimum in the flow for deuterons and Z=2

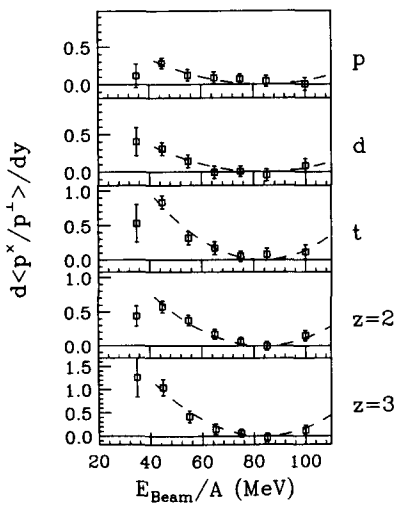

Figure 5: Reduced flow values as a function of incident energy.

fragments and that the remaining fragments are consistent with a minimum occurring around

82 MeV/nucleon.

To gain insight into the interpretation of this value of E_{bal} we have carried out BUU calculations for the system of Ar+V to determine the sensitivity of the model calculations to the EOS and to the nucleon-nucleon cross sections used in the model. In Fig. 6a we show BUU calculations for Ar+V using two different values for the nuclear incompressibility, K.

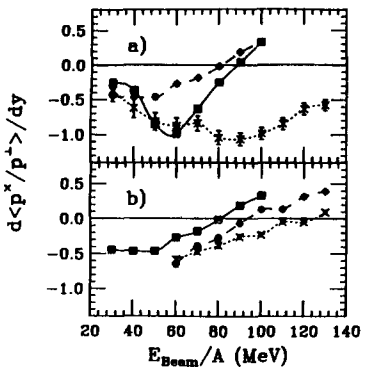

Figure 6: Excitation functions for calculated flow using the BUU model for Ar+V collisions.

The first value of K=200 MeV corresponds to a soft EOS (dashed line) while K=380 MeV represents a stiff EOS (solid line). The predicted E_{bal} changes from 80 MeV/nucleon for K=200 MeV to 88 MeV/nucleon for K=380 MeV. Thus the BUU calculations are sensitive to the EOS but the predicted E_{bal} only changes 10% for a 100% change in the compressibility.

It has been suggested that the nucleon-nucleon scattering cross sections, σ_{nn}, might be lowered in the nuclear medium. The sensitivity to the nucleon-nucleon scattering cross sections in BUU is illustrated in Fig. 6b where the predicted slopes are given for an EOS with K=200 MeV but with three different values of σ_{nn}. The solid line represents 1.0 times the standard energy dependent parameterization of the σ_{nn}. The dashed and dotted lines represent 0.9 and 0.7 times σ_{nn} respectively. The corresponding values of E_{bal} predicted for the three cases of 1.0, 0.9, and 0.7 times σ_{nn} are 80, 96, and 122 MeV/nucleon. Thus the predicted E_{bal} varies 20% for a 10% variation in the assumed σ_{nn}. One may be able to isolate the contribution of σ_{nn} from that of the EOS by studying the mass systematics of E_{bal}. The attractive mean field part of the interaction should scale as the surface, or as $A^{2/3}$, while the the repulsive interaction should scale as the number of collisions, which in turn should be proportional to A, giving an overall decrease in E_{bal} as the mass of the system is increased. The systematic study of E_{bal} as a function of the mass of the system may enable one to determine the σ_{nn} sufficiently well to extract information about the EOS. Our results are consistent with the result that the EOS has K=200 MeV and that σ_{nn} is not modified in the

nuclear medium.

3.3 Multi-fragment emission

Many fragments are emitted in each central collision at intermediate energies. The question of the dynamics of this emission process bears directly on the question of whether the concepts of thermal equilibrium are applicable which in turn determines whether one can extract information about the EOS from these reactions. Two extreme concepts for the emission process of fragments are sequential emission and simultaneous emission. In sequential emission, it is assumed that each observed fragment is emitted singly with the emitting system recoiling and reequilibrating after each particle is emitted. Daughter fragments may also emit sequentially. In simultaneous emission, the system is assumed to disintegrate instantaneously. These two situations will have different kinematic correlations between the emitted fragments. One way to study these correlations was suggested by López and Randrup[20] involving event shape analysis. In this method, each event is characterized using an energy/momentum tensor

$$\mathbf{F}_{ij} = \sum_n \frac{p_i^n p_j^n}{2m_n}. \tag{2}$$

Ordered eigenvalues of $\mathbf{F}$, $f_1 < f_2 < f_3$ are used to define the quantities

$$q_i = \frac{f_i^2}{\sum_{j=1}^3 f_j^2}. \tag{3}$$

In terms of these variables, sphericity and coplanarity are defined as $S = \frac{3}{2}(1 - q_3)$ and $C = \frac{1}{2}\sqrt{3}(q_2 - q_1)$ respectively. López and Randrup demonstrated that by plotting the correlation between these two parameters one could differentiate between the processes of sequential and simultaneous emission.

For sequential processes, emitted fragments will lie near a line corresponding to two-dimensional shapes. The prediction for events exhibiting simultaneous emission will fill more of the available triangular region corresponding to triaxial shapes. Our data for 65 MeV/nucleon Ar+V are shown in Fig. 7.

In order to be able to calculate the effect of sequential and simultaneous emission on the observed distribution of sphericity versus coplanarity, we created a simulation that could reproduce all the simple observables such as multiplicity, energy spectra, and production cross section while providing the opportunity of varying the disassembly dynamics[18]. This simulation proceeds by first obtaining the excitation energy available in the center-of-mass from kinematics and then obtaining a temperature from $E^* = aT^2$ where E^* is the excitation energy, a is the level density parameter, and T is the temperature. Using T the charge and mass of the fragment to be emitted are chosen based on a Boltzmann weighting factor. The

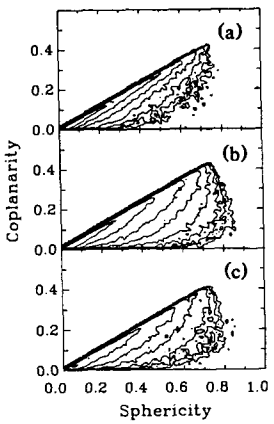

Figure 7: Sphericity versus coplanarity for 65 MeV/nucleon Ar+V. Three contours correspond to a factor of ten in yield.

energy of the fragment is chosen from a Boltzmann distribution and the fragment is emitted with that energy along with a coulomb energy. The remaining excitation energy is shared between the remnant and the emitted fragment using an equal temperature assumption. This sequential emission continues until all fragments have too little energy to emit particles. The simultaneous simulation is created from the events generated using the sequential simulation by randomizing the directions in which the particles are emitted. The results of the simulation are filtered through the acceptance of the 4π Array. Constraints are placed on the simultaneous simulation to account for the possibility that the randomized particles might not be detectable in the 4π Array due to multiple particles striking a single detector and that the multiplicity of observed particles after the filter must still reproduce the measured value. The results of the sequential and simultaneous simulations are compared to the data in Fig. 8 for 65 MeV/nucleon Ar+V. Note that the simultaneous simulation resembles the data more closely than the sequential.

To make a quantitative comparison between the data and the predictions of the simulation, we have extracted the centroids of sphericity and coplanarity for the data and the simulations for the cases of 35 to 85 MeV/nucleon. These results are given in Fig. 9. At 35 MeV/nucleon the data are reproduced by the sequential simulation. As the beam energy is raised, the data agree less with the sequential simulation but do not completely change over to simultaneous emission. These results can be explained by the onset of multifragmentation with the daughter fragments retaining some of their sequential character.

3.4 Azimuthal asymmetries

Another technique that can shed light on the details of the emission of particles from these reactions is azimuthal asymmetries. This method relies on the determination of the

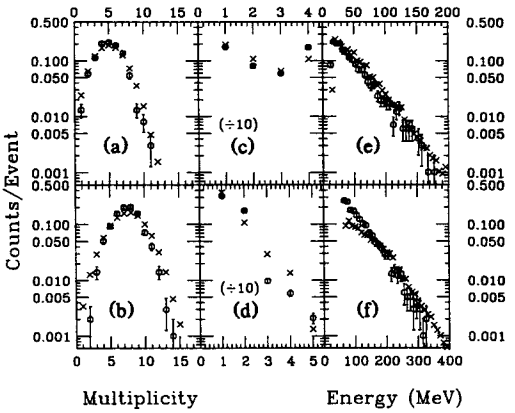

Figure 8: Comparison of the simulation to simple observables for 65 MeV/nucleon Ar+V.

reaction plane. As discussed above, our method of determining the reaction plane allows the observation of rotation-like phenomena that would not have been observed as well using the reaction plane determination techniques previously existing in the literature. Thus we can use the technique of azimuthal asymmetries to study the relative importance of rotation-like phenomena and collective flow that we have seen previously to provide interesting information about the reaction dynamics.

In Fig. 10 the number of particles per unit azimuthal angle with respect to the reaction plane, ϕ, are plotted for H fragments emitted from reactions of 35 MeV/nucleon Ar+V. Note that the peaks at $\phi = 0$ and 180° correspond to emission in the reaction plane. Marked in Fig. 10 are gates in ϕ representing fragments emitted in-plane, out-of-plane, on the projectile side, and on the target side. To characterize fragment emission, we have defined two ratios. The first is the fraction of particles emitted in-plane (± 45°),

$$F_{ip} = \frac{particles\ in-plane}{total\ number\ of\ particles}, \tag{4}$$

and the second is the fraction of particles emitted toward the projectile side (± 45°),

$$F_{ps} = \frac{particles\ on\ the\ projectile\ side}{total\ number\ of\ particles}. \tag{5}$$

Note that a value of 0.5 for either ratio signifies isotropic emission.

The ratio F_{ip} can be related to rotation-like behavior while F_{ps} is related to collective flow. In Fig. 11 these two ratios are plotted for H and He fragments from 35 MeV/nucleon Ar+V

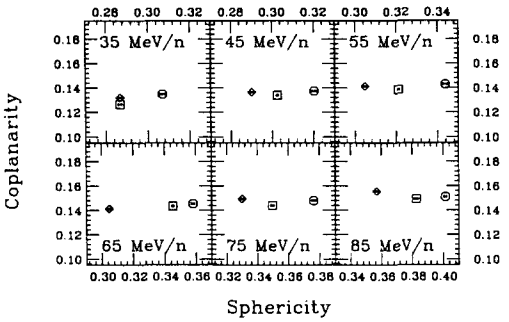

Figure 9: Comparison of the centroids of sphericity and coplanarity between the data and a simulation incorporating sequential and simultaneous emission.

as a function of the rapidity in the laboratory frame. At rapidities near the center-of-mass, F_{ip} is significantly larger than 0.5 and F_{ps} is nearly 0.5. This enhancement for F_{ip}, nearly equal on the projectile and target sides, signifies rotation. At rapidities near the projectile, both ratios approach isotropy for H fragments and are larger than 0.5 for He fragments. This result is consistent with our earlier result that collective flow is stronger for heavier fragments[15,16]. In principle F_{ip} should be symmetric about $y=y_{cm}$ but the acceptance of the 4π Array is not symmetric in the center-of-mass. To study the dependence of F_{ip} on incident energy, a lower rapidity gate for H fragments was chosen where the in-plane enhancement is dominated by rotation. A higher rapidity gate for He fragments was chosen where collective flow dominates. The gates are shown in Fig. 11. The resulting F_{ip} values are shown in Fig. 12 as a function of the incident energy.

At 35 MeV/nucleon, there is a clear signal for rotation-like behavior as indicated by the values of F_{ip} being significantly larger than 0.5 within the lower rapidity gate. As the beam energy is increased, F_{ip} approaches the value of 0.5 signaling that the rotation-like phenomena observed at the lower energies is disappearing and isotropic emission is beginning to dominate. The previously discussed disappearance of flow is illustrated by the trend towards isotropy exhibited by F_{ip} within the higher rapidity gate.

4. CONCLUSIONS

We observed the disappearance of collective flow in Ar+V collisions. The incident energy at which collective flow disappears is the energy at which the attractive scattering, dominant at low energies, changes over to the repulsive scattering observed at high energies. For Ar+V this balance energy is around 82 MeV/nucleon. Previous work has shown that for heavier systems (La+La), the balance energy is below 50 MeV/nucleon[26]. Thus we have indications

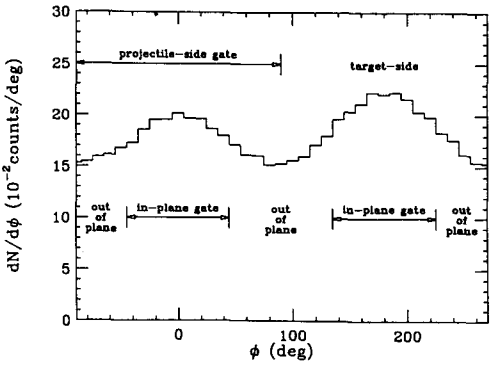

Figure 10: Azimuthal distributions of H fragments from 35 MeV/nucleon Ar+V.

of the mass dependence of E_{bal} with heavier systems having a lower E_{bal} and lighter systems having a higher E_{bal}.

In addition we have presented evidence for the onset of multifragmentation in Ar+V from global event shape analysis in terms of sphericity/coplanarity. The onset seems to occur between 35 and 45 MeV/nucleon in central collisions of Ar+V corresponding to excitation energies between 8 and 10 MeV/nucleon. The data are never described by the completely simultaneous simulation even at the higher energy. The fragment emission seems to retain some of its two-body character. This observation may be explained by realizing that although the primary fragment distribution may be created by an explosion-like mechanism, the resulting fragments may be excited and decay sequentially producing a vestige of the kinematic correlations expected from sequential decay.

We also observed a clear signature for rotation-like phenomena in 35 MeV/nucleon Ar+V reactions. We introduced a new method of determining the reaction plane that can determine the impact vector when rotation or collective flow are present in contrast to the method of Danielewicz and Odyniec in which a reaction plane can not be determined well in the case of where rotation dominates. As the beam energy is increased to 85 MeV/nucleon, this rotation decreases smoothly.

Thus a clear picture of the reaction mechanisms of intermediate heavy ion reactions can be developed. We have evidence that in collisions of Ar+V at 35 MeV/nucleon, we create a long-lived system that emits particles sequentially. These particles also appear to be coming from a rotating source. This rotational behavior is superimposed on collective flow that is dominantly attractive in character. As we raise the incident energy of the incoming Ar nuclei to 100 MeV/nucleon, we see a smooth and qualitative change in these emission patterns. At the highest energy, the emission of fragments is more isotropic and the overall character of

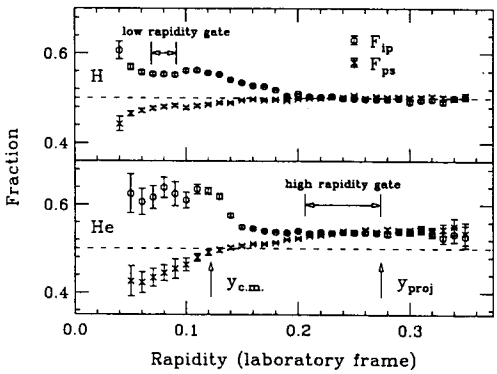

Figure 11: In-plane and projectile ratios for H and He fragments from 35 MeV/nucleon Ar+V.

the collective flow of energy has changed toward repulsive scattering. Most of the rotational behavior has disappeared and the reaction mechanism seems to be more like reactions at several hundred MeV/nucleon incident energy.

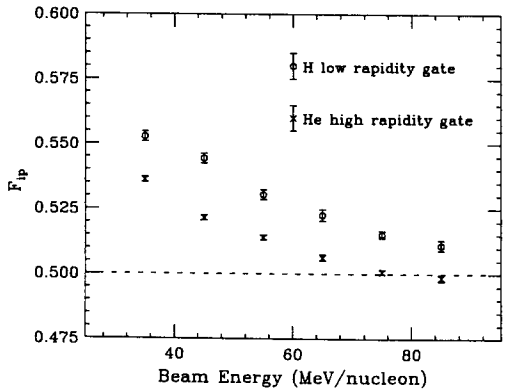

Figure 12: The fraction of particles in-plane for low rapidity H fragments and high rapidity He fragments as a function of incident energy.

REFERENCES

1) M.B. Tsang, R.M. Ronningen, G. Bertsch, Z. Chen, C.B. Chitwood, D.J. Fields, C.K. Gelbke, W.G. Lynch, T. Nayak, J. Pochodzalla, T. Shea, and W. Trautmann, Phys. Rev. Lett. 57 (1986) 559.

2) H.Å. Gustafsson, H.H. Gutbrod, B. Kolb, H. Löhner, B. Ludewigt, A.M. Poskanzer, T. Renner, H. Riedesel, H.G. Ritter, A. Warwick, F. Weik and H. Wieman, Phys. Rev. Lett. 52 (1984) 1590.

3) K. Doss, H.Å. Gustafsson, H. Gutbrod, K. Kampert, B. Kolb, H. Löhner, B.Ludewigt, A.M. Poskanzer, H.G. Ritter, H.R, Schmidt, and H. Wieman, Phys. Rev. Lett. 57 (1986) 302.

4) K. Doss, H.Å. Gustafsson, H. Gutbrod, J. Harris, B. Jacak, K. Kampert, B. Kolb, A. Poskanzer, H. Ritter, H. Schmidt, L. Teitelbaum, M. Tincknell, S. Weiss and H. Wieman, Phys. Rev. Lett. 59 (1987) 2720.

5) H.Å. Gustafsson, H.H. Gutbrod, J. Harris, B.V. Jacak, K.H. Kampert, B. Kolb, A.M. Poskanzer, H.G. Ritter, and H.R. Schmidt, Mod. Phys. Lett. A3 (1988) 1323.

6) P. Danielewicz, H. Ströbele, G. Odyniec, D. Bangert, R. Bock, R. Brockmann, J.W. Harris, H.G. Pugh, W. Rauch, R.E. Renfordt, A. Sandoval, D. Schall, L.S. Schroeder and R. Stock, Phys. Rev. C38 (1988) 120.

7) J. Aichelin and G.F. Bertsch, Phys. Rev. C31 (1985) 1730.

8) H. Kruse, B. Jacak, and H. Stöcker, Phys. Rev. Lett. 54 (1985) 289.

9) H. Kruse, B.V. Jacak, J.J. Molitoris, G.D. Westfall, and H. Stöcker, Phys. Rev. C31 (1985) 1770.

10) J.J. Molitoris, D. Hahn and H. Stöcker, Nucl. Phys. A447 (1986) 13c.

11) G.F. Bertsch, W.G. Lynch and M.B. Tsang, Phys. Lett. 189B (1987) 384.

12) A. Bonasera, L.P. Csernai and B. Schürmann, Nucl. Phys. A476 (1988) 159.

13) G.F. Bertsch and S. Das Gupta, Phys. Rep. 160 (1988) 189.

14) C. Gale, G.M. Welke, M. Prakash, S.J. Lee, and S. Das Gupta, Phys. Rev. C41 (1990) 1545.

15) C.A. Ogilvie, D.A. Cebra, J. Clayton, P. Danielewicz, S. Howden, J. Karn, A. Nadasen, A. Vander Molen, G.D. Westfall, W.K. Wilson, and J.S. Winfield, Phys. Lett. 231B (1989) 35.

16) C.A. Ogilvie, D.A. Cebra, J. Clayton, P. Danielewicz, S. Howden, J. Karn, A. Nadasen, A. Vander Molen, G.D. Westfall, W.K. Wilson, and J.S. Winfield, Phys. Rev. C40 (1989) 2592.

17) C.A. Ogilvie, W. Bauer, D.A. Cebra, J. Clayton, S. Howden, J. Karn, A. Nadasen, A. Vander Molen, G.D. Westfall, W.K. Wilson, and J.S. Winfield, Phys. Rev. C Rapid Communications, in press, 1990.

18) D.A. Cebra, S. Howden, J. Karn, A. Nadasen , C.A. Ogilvie, A. Vander Molen, G.D. Westfall, W.K. Wilson, and J.S. Winfield, Phys. Rev. Lett. 64 (1990) 2246.

19) G. Fai and J. Randrup, Nucl. Phys. A404 (1983) 551.

20) J.A. López and J. Randrup, Nucl. Phys. A491 (1989) 477.

21) W.K. Wilson, W. Benenson, D.A. Cebra, J. Clayton, S. Howden, J. Karn, T. Li, C.A. Ogilvie, A. Vander Molen, G.D. Westfall, J.S. Winfield, B. Young, and A. Nadasen, Phys. Rev. C41 (1990) R1881.

22) G.D. Westfall, J.E. Yurkon, J. van der Plicht, Z.M. Koenig, B.V. Jacak, R.Fox, G.M. Crawley, M.R. Maier, B.E. Hasselquist, R.S. Tickle, and D. Horn, Nucl. Inst. Meth. 238 (1985) 347.

23) C.A. Ogilvie, D.A. Cebra, J. Clayton, S. Howden, J. Karn, A. Vander Molen, G.D. Westfall, W.K. Wilson, and J.S. Winfield, Phys. Rev. C40 (1989) 654.

24) G. Fai and J. Randrup, Comp. Phys. Comm. 42 (1986) 385.

25) P. Danielewicz and G. Odyniec, Phys. Lett. 157B (1985) 146.

26) D. Krofcheck, W. Bauer, G.M. Crawley, C. Djalali, S. Howden, C.A. Ogilvie, A. Vander Molen, G.D. Westfall, and W.K. Wilson, R.S. Tickle, and C. Gale, Phys. Rev. Lett. 63 (1989) 2028.